Neuroscience Letters 668 (2018) 37–42

Contents lists available at ScienceDirect

Neuroscience Letters

journal homepage: www.elsevier.com/locate/neulet

Research article

White matter tractography of the neural network for speech-motor control in children who stutter

Ehsan Misaghi[a,b], Zhaoran Zhang[c], Vincent L. Gracco[d,e], Luc F. De Nil[f], Deryk S. Beal[f,g,*]

[a] Neuroscience and Mental Health Institute, Faculty of Medicine and Dentistry, University of Alberta, Edmonton, AB, Canada
[b] Institute for Stuttering Treatment and Research, Department of Communication Sciences and Disorders, Faculty of Rehabilitation Medicine, University of Alberta, Edmonton, AB, Canada
[c] College of Life Sciences, Sichuan University, Chengdu, Sichuan, China
[d] School of Communication Sciences and Disorders, McGill University, Montreal, QC, Canada
[e] Haskins Laboratories, New Haven, CN, USA
[f] Department of Speech-Language Pathology, Faculty of Medicine, University of Toronto, Toronto, ON, Canada
[g] Bloorview Research Institute, Holland Bloorview Kids Rehabilitation Hospital, Toronto, ON, Canada

ARTICLE INFO

Keywords:
Diffusion tensor imaging (DTI)
Magnetic resonance imaging (MRI)
Deterministic tractography
Developmental stuttering
Speech production
Motor control

ABSTRACT

Stuttering is a neurodevelopmental speech disorder with a phenotype characterized by speech sound repetitions, prolongations and silent blocks during speech production. Developmental stuttering affects 1% of the population and 5% of children. Neuroanatomical abnormalities in the major white matter tracts, including the arcuate fasciculus, corpus callosum, corticospinal, and frontal aslant tracts (FAT), are associated with the disorder in adults who stutter but are less well studied in children who stutter (CWS). We used deterministic tractography to assess the structural connectivity of the neural network for speech production in CWS and controls. CWS had higher fractional anisotropy and axial diffusivity in the right FAT than controls. Our findings support the involvement of the corticostriatal network early in persistent developmental stuttering.

1. Introduction

Stuttering is a neurodevelopmental disorder characterized by sound repetitions, prolongations and silent blocks that impair speech production. The disorder affects 1% of the general population and 5% of children [1]. Stuttering first presents in children aged 18–60 months and progresses along one of two developmental courses: 75% of children experience complete recovery within 2 years of onset, while the disorder persists into adulthood in the opposing 25% of children [2]. Genetic and neural mechanisms have been implicated in the disorder but remain poorly understood [3].

Structural connectivity deficits have been identified throughout the neural network for speech and language function in both children who stutter (CWS) and adults who stutter (AWS). White matter volume of the frontal radiation of the corpus callosum has been found to be lower in CWS than controls in at least one study [4], but findings in the literature are inconsistent with a second study failing to find such a difference [5]. Fractional anisotropy (FA) of the arcuate fasciculus, corpus callosum and corticospinal tract has also been found to be lower in CWS than controls [6,7]. A recent longitudinal study replicated these FA findings and further showed that CWS have reduced FA growth rates in left arcuate fasciculus and corpus callosum relative to controls that were not apparent in children who had recovered from stuttering [8]. Relatedly, people who stutter also have reduced grey matter volume growth rates in the left posterior inferior frontal gyrus (pIFG) relative to controls [9]. The reduced grey matter volume growth rates of the left pIFG documented in people who stutter may be the result of structural connectivity deficits in the corpus callosum and arcuate fasciculus that ultimately limit the region's ability to communicate the critical articulatory coding information to the remainder of the speech neural network in the timely and sequential nature necessary for fluent speech production.

AWS have been shown to have increased white matter volume in the left middle temporal gyrus, right pIFG and right insula [10]. AWS also have lower FA in the white matter underlying the left pIFG, ventral premotor cortex and middle primary motor cortex [11–13], along with a lower cortico-cortical structural connection strength in the left hemisphere relative to controls [12]. As the previously identified

Abbreviations: CWS, children who stutter; AWS, adults who stutter; FAT, frontal aslant tract; CST, corticospinal tract; pIFG, posterior inferior frontal gyrus; SMA, supplementary motor area; DTI, diffusion tensor imaging; FA, fractional anisotropy; MD, mean diffusivity; RD, radial diffusivity; AD, axial diffusivity; PPVT, Peabody Picture Vocabulary Test; SSI, Stuttering Severity Instrument; ROI, region of interest

* Corresponding author at: Bloorview Research Institute Holland Bloorview Kids Rehabilitation Hospital 150 Kilgour Road, M4G 1R8 Toronto, ON, Canada.
E-mail address: dbeal@hollandbloorview.ca (D.S. Beal).

https://doi.org/10.1016/j.neulet.2018.01.009
Received 22 September 2017; Received in revised form 15 December 2017; Accepted 4 January 2018
Available online 05 January 2018
0304-3940/

deficits are clustered around the left pIFG and its white matter tract connections to the ventral premotor and motor cortices, supplementary motor area (SMA) and posterior superior temporal gyrus in people who stutter, we were interested in studying the major tracts that network these nodes. Namely, the major white matter tracts connecting the left pIFG to the neural network for speech production are the arcuate fasciculus, corticospinal tract, corpus callosum and the lesser studied frontal aslant tract (FAT).

The FAT is an obliquely oriented, white matter pathway that connects the pIFG, ventral premotor and motor cortices and SMA and is known to be strongly left lateralized in typical right-handed individuals [14,15]. There is mounting evidence that the structural integrity of the FAT is critical for speech and language function. Structural abnormalities in the FAT are associated with nonfluent primary progressive aphasia (PPA) and are correlated with measures of mean length of utterance and words per minute in patients with PPA [16]. The FAT was recently implicated in persistent developmental stuttering. A study found higher mean diffusivity (MD) in the FAT bilaterally in AWS than controls [17]. To date, the FAT has not been a targeted neuroanatomic structure of interest in structural connectivity studies of CWS, likely due to the lack of sensitivity to this tract by the white matter analysis methods previously employed with the population. Deterministic tractography analysis of diffusion tensor data is a method known to accurately identify FAT.

To address the gap in knowledge regarding the structural integrity of the FAT in CWS and its potential importance for fluent speech production early in stuttering onset, we used deterministic tractography to virtually dissect the FAT and assess its diffusion metrics, as well as the other major white matter tracts that connect the pIFG to the speech neural network, in CWS and matched controls.

2. Materials and methods

2.1. Participants

A total of twenty-two children (11 CWS, 11 controls) ranging from 6 to 12 years of age participated in the study. All of the children were male, right handed as determined by the Edinburgh handedness inventory [18], spoke English as their first language and had a reported negative history for neurological impairments. The CWS ranged in severity from very mild to severe on the Stuttering Severity Instrument – Third Edition (SSI-3) [19]. Inter-rater reliability for the SSI-3 scores was high (ICC = 0.964). All of the children had normal hearing, articulation and receptive vocabulary abilities as screened with a pure-tone hearing test, the Goldman-Fristoe Test of Articulation – Second Edition [20] and the Peabody Picture Vocabulary Test (PPVT) – Third Edition [21]. The two groups did not differ in age and articulation nor receptive vocabulary ability ($p > 0.05$). Table 1 below lists the age, and PPVT and SSI scores of the participants. All participants were able to complete the research protocol. The parents gave informed written consent and the children gave informed assent. The research study was approved by the Toronto Hospital for Sick Children's Research Ethics Board.

Table 1
Summary statistics for participants' age, PPVT-3 and SSI-3 scores.

Group	Parameter	Age (months)	PPVT Score	SSI Score
Controls	Mean	119.18	121.45	N/A
	SD	22.46	11.94	N/A
	Range	74–144	105–138	N/A
CWS	Mean	114.18	118.73	22.09
	SD	18.07	17.26	8.39
	Range	92–148	88–139	7–34

SD: Standard Deviation.

2.2. Data acquisition

The data were collected as part of a larger research protocol that included other experiments for which results are reported elsewhere [4,22]. Pertinent to the current study, neuroanatomical images were acquired from all participants using a 1.5-T Signa Excite III HD 12.0 MRI system (GE Medical Systems, Milwaukee, WI) and an eight-channel head coil. We collected diffusion-weighted data via two runs of a single-shot echo planar imaging (EPI) sequence, each with the same 15 non-collinear directions (TE = 82.3 ms, TR = 17s, matrix size: 128 × 128, FOV: 25 cm, b = 1000 s/mm^2) and 2 b = 0 images. We also collected T1-weighted images using a 3D fast spoiled gradient echo (FSPGR) sequence (flip angle = 15°, TE = 4.2 ms, TR = 9 ms) with 100 1.5-mm-thick axial slices (matrix size: 256 × 192, FOV: 24 cm).

2.3. Tractography and virtual dissection

All of the images were visually inspected, and images corrupted by acquisition errors (e.g., ghosting, missing slices) or extraneous movement [23], were excluded from further analysis. For each participant, we merged the two runs of diffusion images to create datasets with 4 b = 0 and 30 b = 1000 images. Eddy current and motion distortion correction was done using ExploreDTI [24]. To ensure accurate tract dissection, we differed the angle, length and FA values for tractography according to the characteristics of the specific tract under analysis. Tract specific parameters used for tractography are shown in Table 2 [17,25].

2.3.1. Frontal aslant tract (FAT)

The FAT was identified using the method proposed by Catani and colleagues [14]. One of the two regions of interest (ROIs) was placed in the sagittal view encompassing the pIFG and the other one was placed in the superior frontal gyrus encompassing the SMA and pre-SMA (Fig. 1).

2.3.2. Corpus callosum

As shown in Fig. 2, we divided the corpus callosum into three parts based on the proposed scheme of [26]. The genu of the corpus callosum was defined as the anterior ⅙ of the corpus callosum length in the midline, the splenium as the posterior ¼ and the body as the middle portion between the genu and splenium. To delineate the genu of the corpus callosum, an inclusive region of interest (i.e., AND ROI) was placed in the midline encompassing the anterior ⅙ of the corpus callosum width and two origin regions of interest (SEED ROIs) were placed two slices (4 mm) parasagittal to the midline encompassing the same area. In order to prune extraneous fibers, we placed two parasagittal exclusive regions of interest (i.e., NOT ROIs) just lateral to the corticospinal tract. Another NOT ROI was placed in the middle of the corpus callosum width in the coronal view to remove potential backward projections of the fibers that may not be related to the genu. For the splenium, we used the posterior ¼ of the callosal width for the AND ROI in the midline and placed two SEED ROIs two slices parasagittal to the midline. Two NOT ROIs were drawn in the sagittal plane, just lateral to the optic radiations and a NOT ROI was placed in the cerebellum at the level of the pons to prune extraneous fibers that potentially go to the cerebellum. The area in between the AND ROIs placed for the genu

Table 2
Tractography parameters used for different tracts.

Tract	FA Threshold	Angle Limitation	Fiber Length (mm)
Frontal Aslant Tract	0.15	30°	20–500
Corpus Callosum	0.2	30°	50–500
Arcuate Fasciculus	0.2	70°	10–500
Corticospinal Tract	0.2	30°	50–500

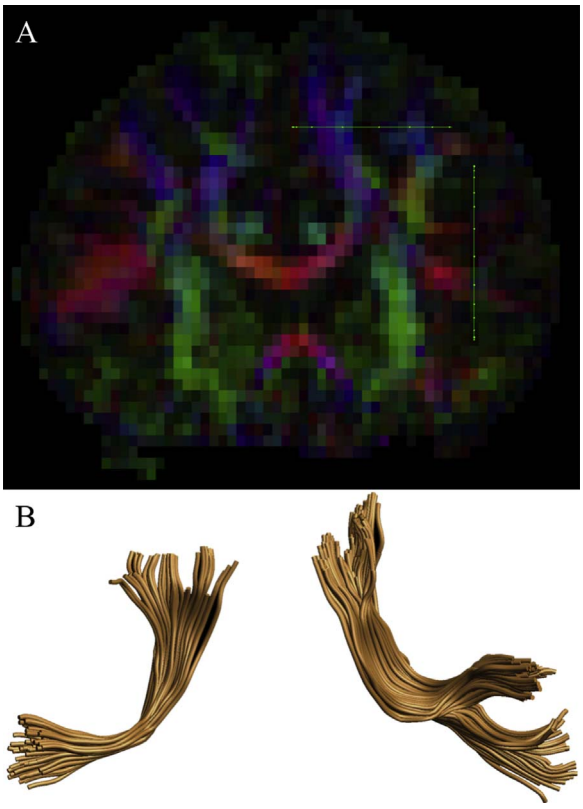

Fig. 1. (A) A coronal view of a representative participant's diffusion image with the ROIs used to extract the FAT delineated in green. Blue fibers and (B) The virtually dissected FAT fibers from a representative participant (radiological convention – left is right). (For interpretation of the references to colour in this figure legend, the reader is referred to the web version of this article.)

and splenium was considered the body and we placed an AND ROI there. Two SEED ROIs were placed two slices parasagittal just as the ones placed for the splenium and genu and two NOT ROIs were placed parasagittal to the corticospinal tract just as the ones placed for the genu. Another NOT ROI was drawn encompassing the whole brain directly under the AND ROI of the midline for the body to remove potential extraneous fibers going in the inferior direction.

2.3.3. Arcuate fasciculus

The arcuate fasciculus was defined in the sagittal plane using the method described by Forkel and colleagues [27]. As shown in Fig. 3, two ROIs were used to delineate the anterior segment of the arcuate fasciculus. We placed one of the two ROIs over the inferior frontal gyrus (ROI 1) and the other one over the supramarginal and angular gyri (ROI 2). The long segment was defined by two ROIs that included the same anterior ROI as the one used to virtually dissect the anterior segment (ROI 1) and a new ROI on Wernicke's area at the level of the posterior superior and middle temporal gyri (ROI 3). The posterior segment was defined using ROI 2 (the posterior ROI of the anterior segment) and ROI 3 (Wernicke's area ROI used in the long segment). The right arcuate fasciculus ROIs were drawn using the same method as its left counterpart.

2.3.4. Corticospinal tract (CST)

The CST was virtually dissected using two AND ROIs, one in the level of the pons encompassing one of the two blue circular areas and the other in the level of the cortex encompassing the dorsal pre- and post-central gyri, known to be the cortical origins of this tract [28]. The left blue circle in the pons in combination with the left cortical ROI was used to delineate the left CST (Fig. 4) and the right counterparts of those areas were used for the right CST.

2.3.5. Inter-rater reliability

Two authors (EM and ZZ) completed the virtual dissection process

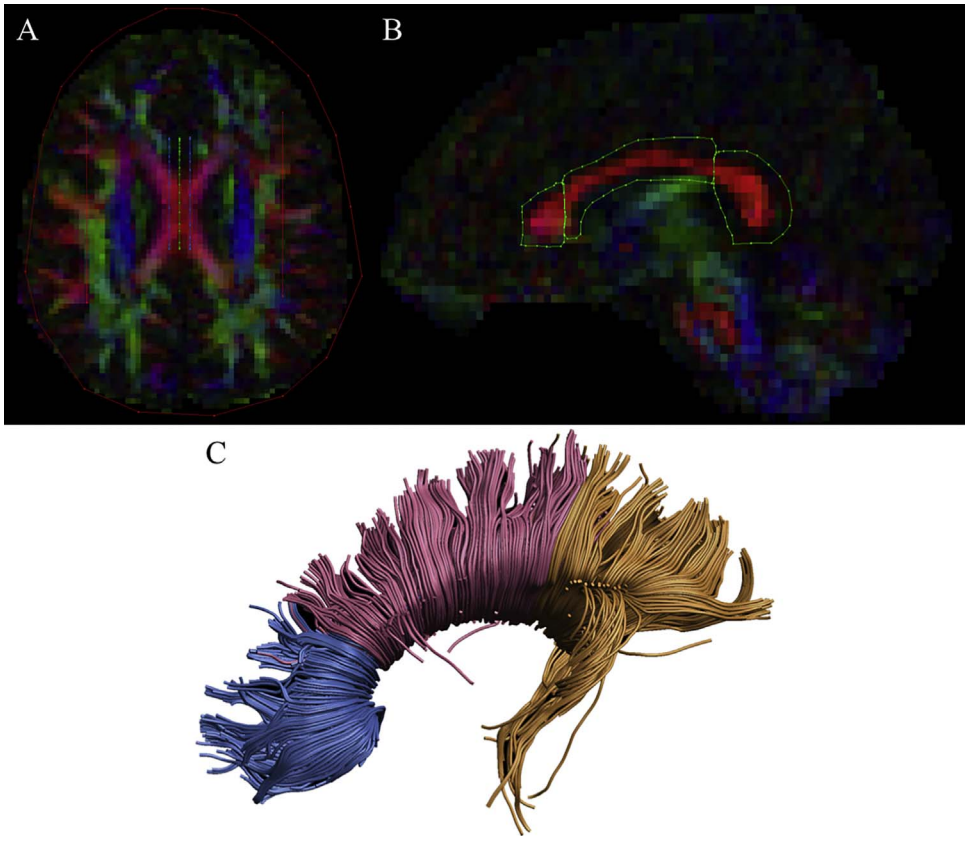

Fig. 2. (A) The ROIs used to delineate the body of the corpus callosum shown on an axial slice of a diffusion image of a representative participant, in the radiological convention. (B) A sagittal view of the AND ROIs for body, genu and splenium of the corpus callosum on a representative participant's diffusion image. (C) An illustration of the corpus callosum in a respresentative participant. Genu, body and splenium fibers are shown in blue, pink and peru colors, respectively. (For interpretation of the references to colour in this figure legend, the reader is referred to the web version of this article.)

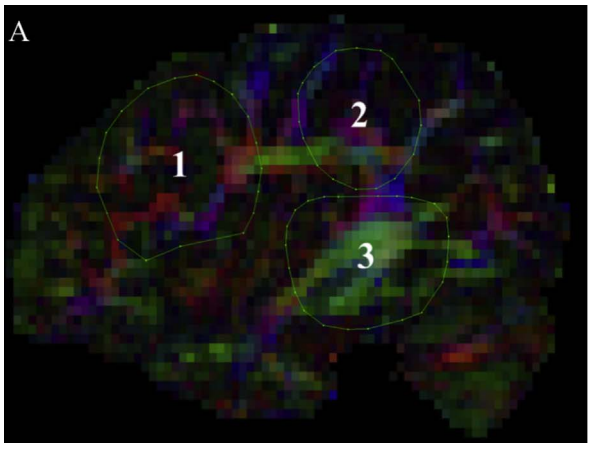

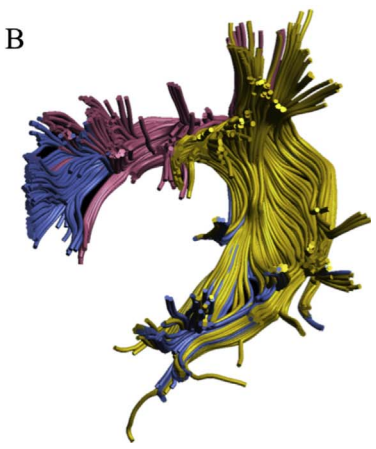

Fig. 3. (A) The sagittal view of the ROIs used to delineate various parts of the arcuate fasciculus on a representative subject's diffusion image. (B) The arcuate fasciculus fibers shown in a representive subject. The long segment is shown in blue, anterior segment in pink and posterior segment in yellow. (For interpretation of the references to colour in this figure legend, the reader is referred to the web version of this article.)

for each tract. Raters were blind to the group membership of the participant for the purpose of virtual dissection. Inter-rater reliability ranged from acceptable to excellent (Table 3). The dissections done by the first author (EM) were considered for this study.

2.4. Statistical analysis

We were able to identify all the tracts in all participants, except the left FAT in one control, and the long segment of the right arcuate fasciculus in another control and two CWS participants. All identified tracts were used in the analysis. We used ExploreDTI to calculate the scalar measurements of the diffusion tensor including FA, mean diffusivity (MD), axial diffusivity (AD) and radial diffusivity (RD) for all the identified tracts. Briefly, FA and RD are positively associated with fiber density and myelination of the white matter tract and therefore structural integrity whereas MD and AD are negatively associated with these white matter properties. The measurements associated with the virtually dissected tracts were exported from ExploreDTI and imported into the IBM SPSS Statistics 22 (IBM Corp. Released 2013. IBM SPSS Statistics for Macintosh, Version 22.0. Armonk, NY) for statistical analyses. Multiple mixed analyses of variance (ANOVA) were performed on FA, MD, AD, RD, and volume of each tract with the hemisphere (left vs. right) as the within-subjects factor and the group (CWS vs. control) the between-subjects factor. Results were accepted as statistically significant if the *p*-value was below the Bonferroni corrected threshold of $p = 0.01$ ($p = 0.05/5$) to account for the 5 variables tested. Post-hoc *t*-tests were used to identify the precise differences when the ANOVA was significant. Bivariate correlations between age, PPVT scores, and SSI scores and the diffusion measures were explored using Pearson's correlation coefficient for the white matter tracts extracted. Due to the exploratory nature of the correlation analyses, results were accepted as statistically significant if the *p*-value was below 0.05 uncorrected for multiple comparisons.

Table 3
ICC Values for the extracted tracts.

Tract		ICC
FAT		0.844
CST		0.950
Corpus Callosum	Genu	0.733
	Body	0.616
	Splenium	0.874
Arcuate Fasciculus	Anterior Segment	0.830
	Long Segment	0.998
	Posterior Segment	0.803

All the ICCs were calculated based on the tract volume.

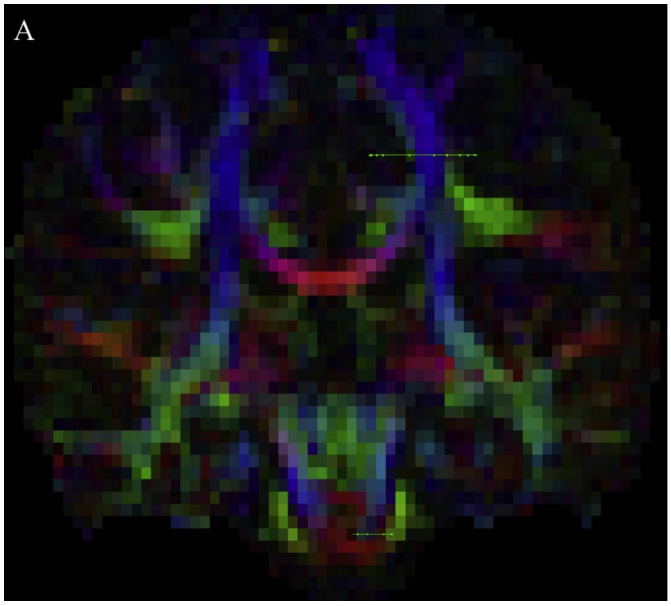

Fig. 4. (A) The ROIs used to extract the corticospinal tract shown on a coronal slice from a representative participant's diffusion image. (B) The bilateral corticospinal tract in a representive participant.

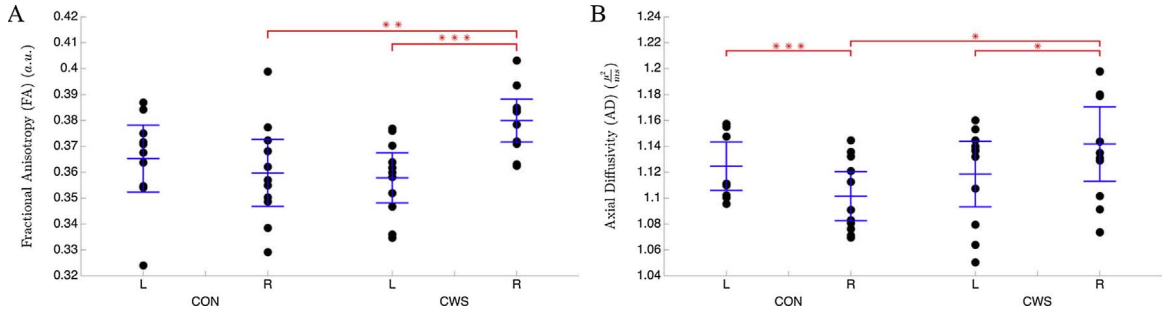

Fig. 5. (A) Fractional anisotropy differences of the frontal aslant tract between and within groups. a.u.: arbitrary units (B) Axial diffusivity differences in the frontal aslant tract between and within groups. *, ** and *** denote significance at the $p < 0.05$, $p < 0.01$ and $p < 0.001$ levels, respectively. The blue lines indicate the 95% confidence interval. CON: Control, CWS: Children Who Stutter. (For interpretation of the references to colour in this figure legend, the reader is referred to the web version of this article.)

3. Results

We observed significant hemisphere by group interactions for FA ($F(1, 19) = 11.179, p = 0.003$) and AD ($F(1, 19) = 21.352, p < 0.0005$) in the FAT. As shown in Fig. 5, the post hoc *t*-tests revealed that FA ($t(20) = -2.93, p = 0.008$) and AD ($t(20) = -2.6, p = 0.017$) of the right FAT were higher in the CWS group relative to that of the control group. Within the CWS group, FA and AD in the right FAT were significantly greater than in the left FAT ($t(10) = -4.718, p < 0.001$ for FA and $t(10) = 2.848, p = 0.017$ for AD) while within the control group, the left FAT had greater AD values than the right FAT ($t(9) = 5.073, p < 0.001$); the opposite direction of that observed in the CWS group. We also observed significant hemisphere main effects for RD ($F(1, 19) = 15.27, p = 0.001$) and tract volume ($F(1, 19) = 10.25, p = 0.005$) in FAT. We did not observe significant group differences in the corpus callosum, arcuate fasciculus and the corticospinal tract. We also found main effects for hemisphere in the CST and AF. For details see supplementary material Table S1. There were no other significant findings.

4. Discussion

We used diffusion tensor imaging, deterministic tractography and virtual dissection to identify and measure the structural integrity of the FAT, for the first time, in CWS. We aimed also to replicate previous findings of white matter abnormalities across the other major tracts underlying the neural network for speech production; namely, the arcuate fasciculus, CST and the corpus callosum. Only diffusion metrics of the FAT differed between the CWS and controls.

As shown in Fig. 5, CWS had greater FA and AD in the right FAT compared to the right FAT in controls thus indicating a high integrity and myelination of these tracts in CWS. Our metrics indicated that the structural integrity and myelination of the right FAT was greater in CWS than controls. The FAT is a major white matter tract connecting the pre-SMA, SMA, pIFG and ventral premotor and motor cortices. Functionally, these regions are known to be a part of the corticostriatal network and are implicated in motor sequencing tasks. Our current results document microstructural abnormalities within this network that have long been implicated in developmental stuttering [29–31]. That CWS had a more highly developed right FAT relative to controls may be related to the beginnings of right hemisphere compensation for subtle abnormalities within the left hemisphere network for motor control, a theory supported by previous behavioral and neuroimaging studies [29,32]. The individual variability of white matter microstructure observed within the CWS in our study may be indicative of the differing states of the structural network relative to the progression of the speech disorder across participants and their varied treatment experiences. One possible interpretation may be that individual CWS with right FAT white matter microstructure most like that of controls' may be poised to shift towards pre-pubescent recovery versus those with more abnormal profiles, but future research will be required to fully explore such an association. Increased white matter density in the right inferior frontal gyrus, a region connected by the FAT to the SMA has been previously reported in AWS [10]. In CWS, the greater the grey matter density of the right inferior frontal gyrus, the greater their speech fluency, or the less severe their stuttering [4]. Furthermore, the left inferior frontal gyrus has been found to develop abnormally over the lifespan of people who stutter spanning in age from 6 to 49 years old [9], while the right inferior frontal gyrus develops along a relatively normal trajectory. Taken together, these findings indicate the importance of the right inferior frontal gyrus and its possible relation to the corticostriatal network to compensate for speech dysfluencies observed in AWS.

Abnormalities of the FAT have been previously reported in AWS. Kronfeld-Duenias and colleagues [17] found that AWS had greater MD in the FAT bilaterally relative to controls. MD is the average diffusivity in all directions of a neural filament. As such, greater MD values indicate compromised structural integrity of the white matter tract. Interestingly, the same authors found that the lower the MD values in the left FAT, the more the speech rate of the AWS approached that of the controls. Our results lend further support to the important role that FAT may have in the generation of fluent speech. Although the characterization of speech dysfluency is different in nonfluent primary progressive aphasia, evidence has shown that diffusion metrics in the left FAT are associated with speech fluency measures in this population. Catani and colleagues [16] reported a negative correlation between RD values and speech fluency, as well as a positive correlation between FA and speech fluency (lexical access) in this patient population. As higher RD typically represents decreased structural integrity of the white matter, and higher FA is associated with greater structural integrity, it is reasonable to conclude that speech fluency is dependent to an extent on the structural integrity of the left FAT. We did not observe any group differences in the left FAT between the CWS and the controls in the current study. The variability in findings in the FAT between children and AWS may represent an abnormal trajectory of white matter development in this tract. Future research should follow CWS longitudinally in an attempt to better understand this phenomenon. Our study found no correlations between stuttering severity and diffusivity metrics.

At least two other studies have reported decreased FA in the posterior part of left arcuate fasciculus of CWS relative to controls as well as in the mid body of the corpus callosum [6,8]. We did not replicate these results in our current findings. A few factors may have contributed to our finding of structural differences confined to the right FAT relative to other studies. We employed a novel methodology relative to the other studies using deterministic tractography to virtually dissect tracts of interest in the speech motor control network versus the whole-brain voxel-based and probabilistic methods used elsewhere. Our measures accounted for characteristics of whole tracts versus that of voxel-sized segments along tracts. Our dataset also examined a modest

sample of school-aged boys with persistent developmental stuttering, across a relatively large age-range for this stage of development, whereas the other studies included a larger sample of children across wider age range and a mixed group of children with recovered and persistent stuttering. Our current results are representative of whole tract measurements in school-aged boys with persistent developmental stuttering.

In summary, we found that CWS had higher FA and AD in the right FAT relative to controls. Unlike previous studies, we did not find microstructure abnormalities in the arcuate fasciculus, corpus callosum or corticospinal tract. Our study used a unique whole-track approach to analysis relative to the voxel-based approaches employed in other studies. As such, we strived to identify robust differences in white matter microstructure along the entirety of a tract rather than those confined to small portions of major tracts detectable at the voxel level. Our findings contribute to the literature supporting an association between persistent developmental stuttering and abnormalities throughout the corticostriatal circuit. Many functional neuroimaging studies have found increased activation of right hemisphere speech regions in people who stutter relative to controls, suggesting hemispheric compensation for a left hemisphere deficit [31,33–35]. We speculate that the abnormal hemispheric dominance of FAT development in our group of CWS may be the beginnings of early compensation for deficits within speech neural network, such as the abnormal trajectory of gray matter development in left inferior frontal gyrus [4,9].

Conflicts of interest

The authors declare that they do not have any conflicting interests.

Disclosures

All procedures performed in this study involving human participants were in accordance with the ethical standards of the institutional and/or national research committee and with the 1964 Helsinki declaration and its later amendments or comparable ethical standards. Informed consent/assent was obtained from all individual participants included in the study.

Acknowledgements

Our research was supported by the Canadian Institutes of Health Research (M0P-68969) to LFD and by the National Institute on Deafness and Other Communication Disorders (R01-DC-007603) to VLG. DSB received funding from the Canadian Institutes of Health Research Clinical Fellowship and the Clinician Scientist Training Program (CSTP). The CSTP is funded fully or in part by the Ontario Student Opportunity Trust Fund and the Hospital for Sick Children Foundation Student Scholarship Program.

Appendix A. Supplementary data

Supplementary data associated with this article can be found, in the online version, at https://doi.org/10.1016/j.neulet.2018.01.009.

References

[1] O. Bloodstein, N.B. Ratner, A Handbook on Stuttering, Thomson Delmar Learning, 2008.
[2] E. Yairi, N.G. Ambrose, Early childhood stuttering I: persistency and recovery rates, J. Speech Lang. Hear. Res. 42 (1999) 1097–1112.
[3] S.J. Kraft, E. Yairi, Genetic bases of stuttering: the state of the art, 2011, Folia Phoniatr. Logop. 64 (2012) 34–47.
[4] D.S. Beal, V.L. Gracco, J. Brettschneider, R.M. Kroll, L.F. De Nil, A voxel-based morphometry (VBM) analysis of regional grey and white matter volume abnormalities within the speech production network of children who stutter, Cortex 49 (2013) 2151–2161.
[5] A.L. Choo, S.E. Chang, H. Zengin-Bolatkale, N.G. Ambrose, T.M. Loucks, Corpus callosum morphology in children who stutter, J. Commun. Disord. 45 (2012) 279–289.
[6] S.E. Chang, K.I. Erickson, N.G. Ambrose, M.A. Hasegawa-Johnson, C.L. Ludlow, Brain anatomy differences in childhood stuttering, Neuroimage 39 (2008) 1333–1344.
[7] S.E. Chang, D.C. Zhu, A.L. Choo, M. Angstadt, White matter neuroanatomical differences in young children who stutter, Brain 138 (2015) 694–711.
[8] H.M. Chow, S.E. Chang, White matter developmental trajectories associated with persistence and recovery of childhood stuttering, Hum. Brain Mapp. 38 (7) (2017) 3345–3359.
[9] D.S. Beal, J.P. Lerch, B. Cameron, R. Henderson, V.L. Gracco, L.F. De Nil, The trajectory of gray matter development in Broca's area is abnormal in people who stutter, Front. Hum. Neurosci. 9 (2015) 89.
[10] D.S. Beal, V.L. Gracco, S.J. Lafaille, L.F. De Nil, Voxel-based morphometry of auditory and speech-related cortex in stutterers, Neuroreport 18 (2007) 1257–1260.
[11] M. Sommer, M.A. Koch, W. Paulus, C. Weiller, C. Buchel, Disconnection of speech-relevant brain areas in persistent developmental stuttering, Lancet 360 (2002) 380–383.
[12] S. Cai, J.A. Tourville, D.S. Beal, J.S. Perkell, F.H. Guenther, S.S. Ghosh, Diffusion imaging of cerebral white matter in persons who stutter: evidence for network-level anomalies, Front. Hum. Neurosci. 8 (2014) 54.
[13] E.L. Connally, D. Ward, P. Howell, K.E. Watkins, Disrupted white matter in language and motor tracts in developmental stuttering, Brain Lang. 131 (2014) 25–35.
[14] M. Catani, F. Dell'acqua, F. Vergani, F. Malik, H. Hodge, P. Roy, R. Valabregue, M. Thiebaut de Schotten, Short frontal lobe connections of the human brain, Cortex 48 (2012) 273–291.
[15] M. Catani, S. Budisavljević, Chapter 22 – contribution of diffusion tractography to the anatomy of language, in: H. Johansen-Berg, T.E.J. Behrens (Eds.), Diffusion MRI, second edition, Academic Press, San Diego, 2014, pp. 511–529.
[16] M. Catani, M.M. Mesulam, E. Jakobsen, F. Malik, A. Martersteck, C. Wieneke, C.K. Thompson, M. Thiebaut de Schotten, F. Dell'Acqua, S. Weintraub, E. Rogalski, A novel frontal pathway underlies verbal fluency in primary progressive aphasia, Brain 136 (2013) 2619–2628.
[17] V. Kronfeld-Duenias, O. Amir, R. Ezrati-Vinacour, O. Civier, M. Ben-Shachar, The frontal aslant tract underlies speech fluency in persistent developmental stuttering, Brain Struct. Funct. 221 (2016) 365–381.
[18] R.C. Oldfield, The assessment and analysis of handedness: the Edinburgh inventory, Neuropsychologia 9 (1971) 97–113.
[19] G.D. Riley, SSI-3, Pro-Ed, 1994.
[20] R. Goldman, Examiner's Manual for the Goldman Fristoe Test of Articulation, NCS Pearson, Inc., Minneapolis, MN, 2000.
[21] L.M. Dunn, L.M. Dunn, PPVT-III. Peabody Picture Vocabulary Test, American Guidance Service Circle Pines, MN, 1997.
[22] D.S. Beal, M.A. Quraan, D.O. Cheyne, M.J. Taylor, V.L. Gracco, L.F. De Nil, Speech-induced suppression of evoked auditory fields in children who stutter, Neuroimage 54 (2011) 2994–3003.
[23] J.D. Tournier, S. Mori, A. Leemans, Diffusion tensor imaging and beyond, Magn. Reson. Med. 65 (2011) 1532–1556.
[24] A. Leemans, B. Jeurissen, J. Sijbers, D. Jones, 17th Annual Meeting of Intl Soc Mag Reson Med, ExploreDTI: a graphical toolbox for processing, analyzing, and visualizing diffusion MR data, Vol. 209 2009, p. 3537.
[25] S. Wakana, A. Caprihan, M.M. Panzenboeck, J.H. Fallon, M. Perry, R.L. Gollub, K. Hua, J. Zhang, H. Jiang, P. Dubey, A. Blitz, P. van Zijl, S. Mori, Reproducibility of quantitative tractography methods applied to cerebral white matter, Neuroimage 36 (2007) 630–644.
[26] S. Hofer, J. Frahm, Topography of the human corpus callosum revisited–comprehensive fiber tractography using diffusion tensor magnetic resonance imaging, Neuroimage 32 (2006) 989–994.
[27] S.J. Forkel, M. Thiebaut De Schotten, F. Dell'Acqua, L. Kalra, D.G.M. Murphy, S.C.R. Williams, M. Catani, Anatomical predictors of aphasia recovery: a tractography study of bilateral perisylvian language networks, Brain 137 (2014) 2027–2039.
[28] A. Kumar, C. Juhasz, E. Asano, S.K. Sundaram, M.I. Makki, D.C. Chugani, H.T. Chugani, Diffusion tensor imaging study of the cortical origin and course of the corticospinal tract in healthy children, AJNR Am. J. Neuroradiol. 30 (2009) 1963–1970.
[29] P.A. Alm, Stuttering and the basal ganglia circuits: a critical review of possible relations, J. Commun. Disord. 37 (2004) 325–369.
[30] S. Smits-Bandstra, L.F. De Nil, Sequence skill learning in persons who stutter: implications for cortico-striato-thalamo-cortical dysfunction, J. Fluency Disord. 32 (2007) 251–278.
[31] A.L. Giraud, K. Neumann, A.C. Bachoud-Levi, A.W. von Gudenberg, H.A. Euler, H. Lanfermann, C. Preibisch, Severity of dysfluency correlates with basal ganglia activity in persistent developmental stuttering, Brain Lang. 104 (2008) 190–199.
[32] S. Brown, R.J. Ingham, J.C. Ingham, A.R. Laird, P.T. Fox, Stuttered and fluent speech production: an ALE meta-analysis of functional neuroimaging studies, Hum. Brain Mapp. 25 (2005) 105–117.
[33] C.A. Kell, K. Neumann, K. von Kriegstein, C. Posenenske, A.W. von Gudenberg, H. Euler, A.L. Giraud, How the brain repairs stuttering, Brain 132 (2009) 2747–2760.
[34] P.T. Fox, R.J. Ingham, J.C. Ingham, T.B. Hirsch, J.H. Downs, C. Martin, P. Jerabek, T. Glass, J.L. Lancaster, A PET study of the neural systems of stuttering, Nature 382 (1996) 158–161.
[35] L.F. De Nil, R.M. Kroll, S. Kapur, S. Houle, A positron emission tomography study of silent and oral single word reading in stuttering and nonstuttering adults, J. Speech Lang. Hear. Res. 43 (2000) 1038–1053.